Particle Swarm-Based Sliding Mode Controller with Chattering Reduction Feature: Application to an AGC Nonlinear Interconnected Model

Al-Hamouz, Z.*, Al-Duwaish, H.**, and Al-Musabi, N.***

**Corresponding Author:* Depeartment of Electrical Engineering
KFUPM, P.O.Box 683, Dhahran 31261, KSA
(Tel: +966 3 860 2782; Fax +966 3 860 3535, e-mail: zhamouz@kfupm.edu.sa)
** Depeartment of Electrical Engineering
KFUPM, P.O.Box 677, Dhahran 31261, KSA (e-mail: hduwaish@kfupm.edu.sa)
*** Electrical Engineering Department, Petroleum Institute,
Abu Dhabi, UAE, (e-mail: nalmusabi@pi.ac.ae)

Abstract ¾ This paper presents a design of a sliding mode controller (SMC) with chattering reduction feature applied to interconnected Automatic Generation Control (AGC) model. The proposed method formulates the design of SMC as an optimization problem and utilizes Particle Swarm Optimization (PSO) algorithm to find the optimal feedback gains and switching vector values of the controller. Two performance functions were used in the optimization process to demonstrate the system dynamical performance and SMC chattering reduction. The tested two-area interconnected AGC model incorporates nonlinearities in terms of Generation Rate Constraint (GRC). Comparison with a previous AGC method reported in literature validates the significance of the proposed SMC design.

Index Terms ¾ Sliding mode control (SMC), Automatic generation control (AGC), Particle Swarm Optimization (PSO), Linear quadratic regulators(LQR), Chattering reduction, Power systems.

1. Introduction

The Automatic Generation Control (AGC) problem has been one of the most important issues in the operation and design of contemporary electric power systems. This importance is due to the role of the AGC in securing a satisfactory operation of power systems and ensuring constancy of speed for induction and synchronous motors, thereby improving the performance of generating units (Kundur, 1994). The purpose of AGC is to track load variation while maintaining system frequency and tie line power interchanges (for interconnected areas) close to specified values. In this way, transient errors in frequency and tie line power should be minimized and steady error should not appear.

In the last two decades, many techniques were proposed for the supplementary control of AGC systems (Kumar and Kothari, 2005). Conventionally, PI and PID controllers are used for AGC (Elgerd and Fosha, 1970; Nanda and Kaul, 1978; Moon et al., 1999; Velusami and Chidambaram, 2006). However, PI has many drawbacks, some of which are long settling time and relatively large overshoots in the transient frequency deviations. Furthermore, utilization of optimal control theory was examined (Glover and Schweppa, 1972; Bengiamin and Chan, 1978). The controller design is normally based on the parameters of the linear incremental model of the power system which, in turn, depend on the condition of the power system. Therefore, the linear optimal controller is sensitive to variations in the plant parameters or operating conditions of the power system. Moreover, the linear optimal controller yields unsatisfactory dynamic response in the presence of Generation Rate Constraint (GRC) (Chan and Hsu, 1981). Other techniques used for designing the secondary control loop for the AGC include Neural Network methods (Beaufays et al., 1994; Demiroren at al., 2001). Superconducting Magnetic Energy Storage (SMES) unit applications (Demiroren at al., 2003) and spline techniques (Rekpreedapong and Feliachi, 2003). Furthermore, the application of SMC to the AGC

problem was considered by many authors (Chan and Hsu, 1981; Demiroren at al., 2001, 2003; Rekpreedapong and Feliachi, 2003, Sivarmakrishnan et al., 1984; Al-Hamouz et al., 2000, 2005, 2007; Al-Musabi et al., 2003). SMC possess some attractive features; mainly robustness and good transient response. In the work of Chan and Hsu (1981), a SM controller was compared with conventional and optimal control methods for two equal-area non-reheat and reheat thermal systems. However, a systematic method for obtaining the switching vector and optimum feedback gain of the SMC was not discussed. Pole placement technique was utilized in designing the SMC for a single area non-reheat AGC system in the work of Sivarmakrishnan et al. (1984). The feedback gains were selected by trial and error.

In practice, AGC models are nonlinear. Unfortunately, conventional control design methods are not efficient when nonlinearities are introduced to the incremental models of control systems. Thus, other methods should be utilized for the design of the controllers. One of the most reliable techniques is the iterative heuristic optimization algorithms which can be used to tune the controllers to obtain their optimum settings. Some of the recent attempts which utilized the iterative heuristic algorithms for solving the AGC problems (for linearized models) can be found in the work of Al-Hamouz et al. (2000) where Genetic Algorithm (GA) was used to optimize only the feedback gains of the SMC applied to a single area non-reheat AGC.On the other hand, in the work of Al-Musabi et al. (2003), PSO was used for the same purpose and for a single area linear model, too. In both works of Al-Hamouz et al. (2000) and Al-Musabi et al. (2003), the switching vector was obtained from another design method reported in literature.

As an extension of the authors' work in Al-Hamouz et al. (2005, 2007), the present paper proposes a design of the whole sliding mode automatic generation controller parameters optimally (both the feedback gains and the switching vectors) using the PSO.

The proposed controller will be applied to a two- areas interconnected nonlinear AGC system. The new SMC design is characterized by chattering reduction feature. This has been accomplished by using a performance function that minimizes the controller effort as will be discussed in section four. The dynamical behavior of the controlled system will be compared to a method reported in literature.

The organization of this paper will be as follows: First, an explanation of a nonlinear AGC model will be presented in section 2 followed by a brief introduction to the SMC theory and PSO algorithm in section 3. The proposed design of SMC using PSO is explained in section 4. Simulations results and comparison with a AGC design method reported in literature is presented in section 5. Finally, conclusions are presented in section 6.

2. Nonlinear Model of Interconnected Power Systems

For two areas interconnected AGC nonlinear power systems, the studied model is shown in Fig. 1 (Yang and Cimen, 1996).

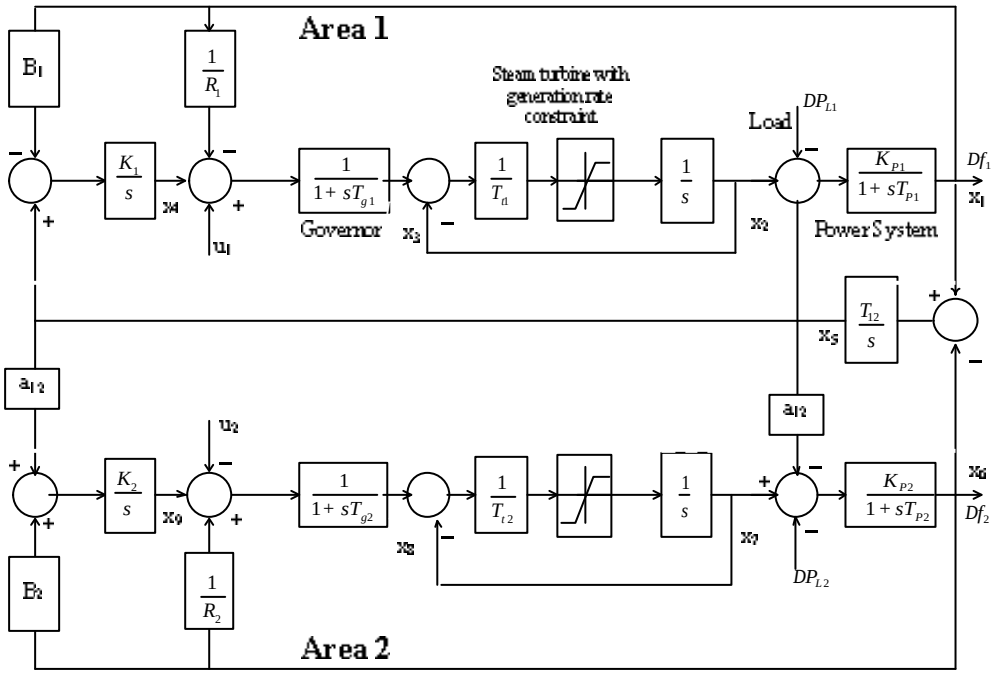

The model includes the effect of Generation Rate Constraint (GRC) and limits on the position of the governor valve, which are caused by the mechanical and thermodynamic constraints in practical steam turbines systems (Chan and Hsu, 1981). GRC imposes limits on the rate of change of generated power. A typical value of 0.015 p.u./min has been included in the model. T_p is the plant model time constant, T_t is the turbine time constant, T_g is the governor time constant, K_p (Hz/p.u. MW) is the plant gain, K is the integral control gain, and R (Hz/ p.u. MW) is the speed regulation due to governor action. x_2 , x_3, and x_4 are respectively the incremental changes in generator output (p.u. MW) , governor valve position (p.u. MW) and integral control of area 1. The tie line power is x_5. On the other hand, x_7 , x_8, and x_9 are respectively the incremental changes in generator output (p.u. MW) , governor valve position (p.u. MW) and integral control of area 2. The control objective in the AGC problem is to keep the change in frequencies (Hz) $\Delta f_1 = x_1$ and $D f_2 = x_6$, as well as the change in tie-line power $\Delta P_{tie} = x_9$ as close to zero as possible when the system is subjected to load disturbance $D P_{L1}$ and $D P_{L2}$ by manipulating the inputs u_1 and u_2, respectively. The values of the parameters used for the interconnected system are as in Table 1.

Table 1: Interconnected system parameters

$T_{P1}=T_{p2}=20$s	$K_{p1}=K_{p2}=120$ Hz p.u. MW^{-1}
$T_{t1}=T_{t2}=0.3$s	$K_1=K_2=1$ p.u. MW rad^{-1}
$T_{g1}=T_{g2}=0.08$s	$R_1=R_2=2.4$ Hz p.u. MW^{-1}
$B_1=B_2=0.425$ p.u.MW/Hz	$T_{12}=0.545$ p.u. MW
$a_{12}=-1$	*GRC (Generation rate constraint)*$=0.015$

3. Overview of SMC and PSO

3.1 Theory of SMC

The fundamental theory of SMC may be found in (Itkis, 1976). Different control goals such as stabilization, tracking, regulation can be achieved using SMC by the proper design of the sliding surface. The discussion here will be limited to the regulation problem where the objective is to keep specified states as close to zero as possible. A block diagram of the SMC for the regulation problem is shown in Fig. 2.

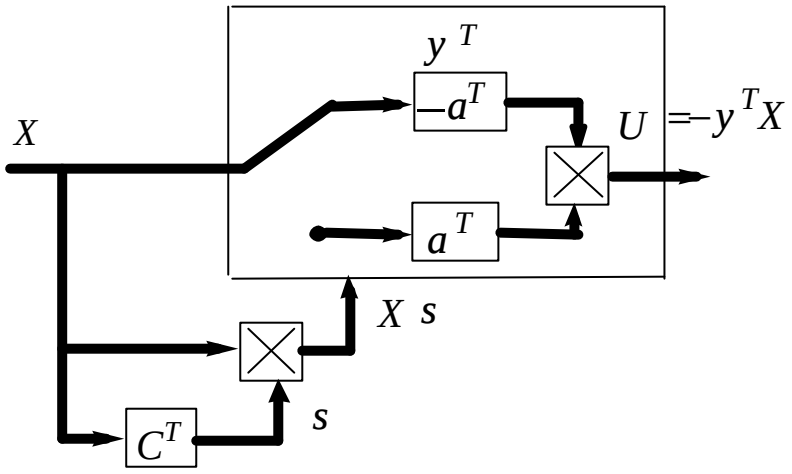

Fig. 2: Block diagram of sliding mode controller (SMC)

The control law is a linear state feedback whose coefficients are piecewise constant functions. Consider the linear time-invariant controllable system given by

$$\dot{X}(t) = AX(t) + BU(t) \tag{1}$$

Where

$X(t)$ n-dimensional state vector

U (t) m-dimensional control force vector

A $n \times n$ system matrix

B $n \times m$ input matrix

The SMC control laws for the system of (1) are given by

$$u_i = -y_i^T X = -\sum_{j=1}^{n} y_{ij} x_j ; i = 1,2,...., m \tag{2}$$

Where the feedback gains are given as

$$y_{ij} = \begin{cases} a_{ij}, \ if \ x_i s_j \rangle 0 \\ \\ -a_{ij}, \ if \ x_j s_i \langle 0 \end{cases} \quad i = 1,....., m; \ j = 0,....., n$$

and

$$s_i(X) = C_i^T X = 0, \qquad i = 1,....,m \tag{3}$$

Where C_i's are the switching vectors which are selected by pole placement or linear optimal control theory.

The design procedure for selecting the constant switching vectors C_i using pole placement is described below.

Step1: Define the coordinate transformation

$$\boldsymbol{Y = MX} \tag{4}$$

such that

$$MB = \begin{bmatrix} 0 \\ .... \\ B_2 \end{bmatrix} \tag{5}$$

where M is a nonsingular $n \times n$ matrix and B_2 is a nonsingular $m \times m$ matrix.

From (4) and (5)

$$\dot{Y} = M\dot{X} = MAM^{-1}Y + MBU \tag{6}$$

Equation (6) can be written in the form

$$\begin{bmatrix}\dot{Y}_1\\ \dot{Y}_2\end{bmatrix}=\begin{bmatrix}A_{11}A_{12}\\ A_{21}A_{22}\end{bmatrix}\begin{bmatrix}Y_1\\ Y_2\end{bmatrix}+\begin{bmatrix}0\\ B_2\end{bmatrix}U \tag{7}$$

where A_{11}, A_{12}, A_{21}, A_{22} are respectively (n-m)×(n-m), (n-m)×m, m×(n-m) and (m×m) submatrices. The first equation of (7) together with (3) specifies the motion of the system in the sliding mode that is

$$\dot{Y}_1 = A_{11}Y_1 + A_{12}Y_2 \tag{8}$$

$$\sum(Y) = C_{11}Y_1 + C_{12}Y_2 \tag{9}$$

where C_{11} and C_{12} are m×(n-m) and (m×m) matrices, respectively satisfying the relation

$$[C_{11}C_{12}] = C^T M^{-1} \tag{10}$$

Equations (8) and (9) uniquely determine the dynamics in the sliding mode over the intersection of the switching hyper-planes

$$s_i(X) = C_i^T X = 0, \qquad i = 1,\ldots,m$$

The subsystem described by (8) may be regarded as an open loop control system with state vector Y_1 and control vector Y_2 being determined by (9), that is

$$Y_2 = -C_{12}^{-1}C_{11}Y_1 \tag{11}$$

Consequently, the problem of designing a system with desirable properties in the sliding mode can be regarded as a linear feedback design problem. Therefore, it can be assumed, without loss of generality, that C_{12} = identity matrix of proper dimension.

Step 2: Equations (8) and (11) can be combined to obtain

$$\dot{Y}_1 = [A_{11} - A_{12}C_{11}]Y_1 \tag{12}$$

Utkin and Yang (1978) have shown that if the pair (A, B) is controllable, then the pair (A_{11}, A_{12}) is also controllable. If the pair (A_{11}, A_{12}) is controllable, then the eigenvalues of the matrix $[A_{11} - A_{12}C_{11}]$ in the sliding mode can be placed arbitrarily by

suitable choice of C_{11}. The feedback gains a_{ij} are usually determined by simulating the control system and trying different values until satisfactory performance is obtained.

3.2 Overview of PSO

Particle Swarm Optimization (PSO) is an evolutionary computation technique developed by Eberhart and Kennedy (1995) inspired by social behaviour and bird flocking or fish schooling. The PSO algorithm applied in this study is shown in the flow-chart of Figure 3.

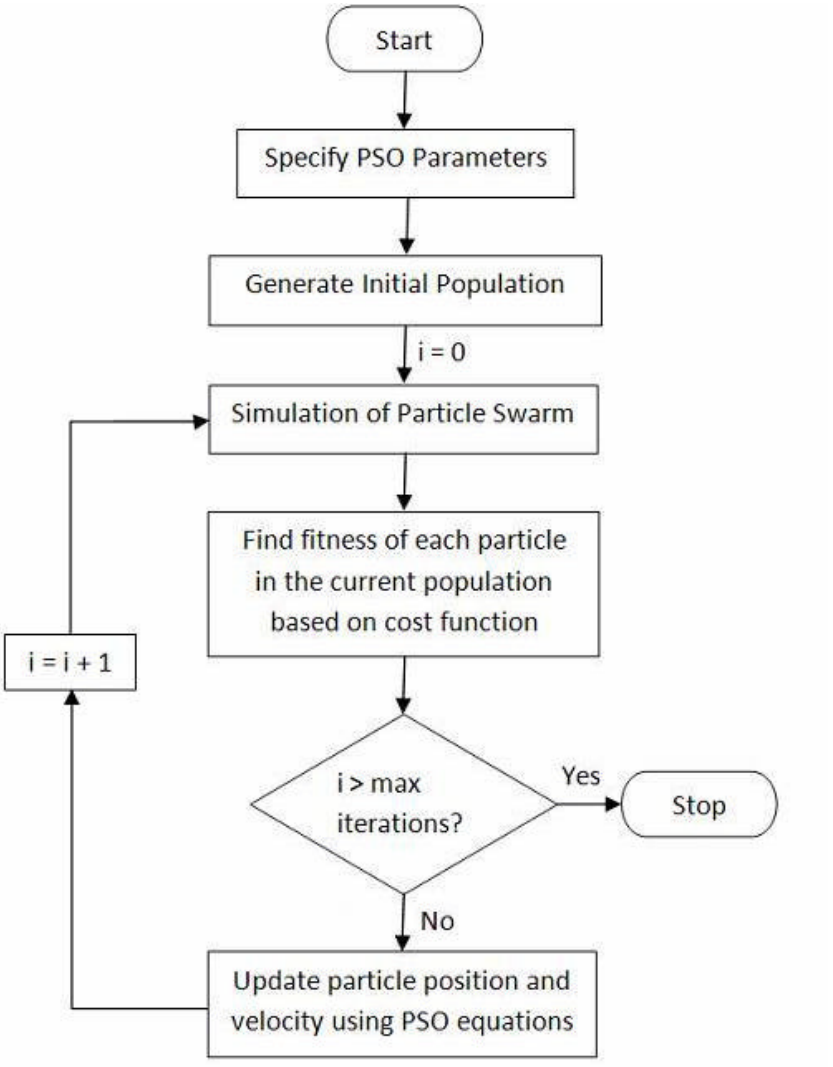

Fig. 3: Flow-chart of particle swarm optimization

The steps of the PSO algorithm can be described briefly as follows

1) Initialize a population (array) of particles with random positions and velocities v on d dimension in the problem space. The particles are generated by randomly selecting a value with uniform probability over the d^{th} optimized search space $[x_d^{\min}, x_d^{\max}]$. Set the time counter t = 0.

2) For each particle x, evaluate the desired optimization fitness function, J, in d variables.

3) Compare particles fitness evaluation with x_{pbest}, which is the particle with best local fitness value. If the current value is better than that of x_{pbest}, then set x_{pbest} equal to the current value, and x_{pbest} locations equal to the current locations in d-dimensional space.

4) Compare fitness evaluation with population overall previous best. If current value is better than *gbest*, the global best fitness value, then reset x_{gbest} to the current particle's array index and value.

5) Update the time counter t, inertia weight w, velocity v, and position of x according to the following equations

$$t = t + 1 \tag{13}$$

$$w(t) = w_{min} + (w_{max} - w_{min}\left(\frac{m - t}{m - 1}\right)) \tag{14}$$

$$v_{id}(t) = w(t)\, v_{id}(t-1) + 2\, a\, (x_{idpbest}(t-1) - x_{id}(t-1)) + 2a\, (x_{idgbest}(t-1) - x_{id}(t-1)) \tag{15}$$

$$x_{id}(t) = v_{id}(t) + x_{id}(t-1) \tag{16}$$

where w_{min} and w_{max} are the maximum and minimum values of the inertia weight w, m is the maximum number of iterations, i is the number of the particles that goes from 1 to n, d is the dimension of the variables, and a is a uniformly distributed random number in (0,1).

The particle velocity in the dth dimension is limited by some maximum value $v_d^{\max}$. This limit improves the exploration of the problem space. In this study, $v_d^{\max}$ is proposed as

$$v_d^{max} = k\, x_d^{max} \tag{17}$$

where k is a small constant value chosen by the user, usually between 0.1-0.2 of x_d^{max}.

6) Loop to 2, until a criterion is met ,usually a good fitness value or a maximum number of iterations (generations) m is reached.

4. PSO-Based Design Approach

The nonlinear interconnected AGC model described in section 2 has 9 state variables and 2 control inputs. The switching vector of the proposed sliding mode controller will be represented by:

$$C^T = \begin{bmatrix} c_{11} & c_{12} & c_{13} & c_{14} & c_{15} & c_{16} & c_{17} & c_{18} & c_{19} \\ c_{21} & c_{22} & c_{23} & c_{24} & c_{25} & c_{26} & c_{27} & c_{28} & c_{29} \end{bmatrix}$$

and the feedback gains are given by:

$$a = \begin{bmatrix} a_{11} & a_{12} & a_{13} & a_{14} & a_{15} & a_{16} & a_{17} & a_{18} & a_{19} \\ a_{21} & a_{22} & a_{23} & a_{24} & a_{25} & a_{26} & a_{27} & a_{28} & a_{29} \end{bmatrix}$$

This will result in a total of 36 parameters to be optimized using the proposed PSO based approach. The following systematic procedure describes the PSO-based design approach for the optimal selection of the feedback gains and switching vectors:

1) Generate randomly a set of possible feedback gains represented by $a_{11},\ldots,a_{21}$ and switching vector $c_{11},\ldots,c_{21}$.

2) Simulate the system in Figure 1 after applying a step load disturbance at ΔP_{L1} and record $\Delta w_1(t)$, $\Delta w_2(t)$ and $\Delta P_{tie}(t)$ for the entire simulation time.

3) Evaluate a performance index for the feedback gains $a_{11},\ldots,a_{21}$ and switching vector values $c_{11},\ldots,c_{21}$ generated in step 1. In the present work, the following performance index is adopted, which has been used by Yang and Cimen (1996):

$$J_1 = \int_0^\infty 0.75\, t|\Delta w_1| + t|\Delta w_2| + 0.5t|\Delta P_{tie}|dt \qquad (18)$$

This selection has been made in order to make it possible for a fair comparison between the performance of the proposed algorithm and that reported in the literature by Yang and Cimen (1996). This performance index emphasizes on improving the dynamical behavior of the AGC system. This has been done by including the absolute error time of the internal parameters of the AGC system into the performance index. Furthermore, to reduce chattering from the control signal, the present paper proposes a second performance index J_2, which includes the deviation of the control effort:

$$J_2 = \int_0^\infty \Delta w_1^{\,2} + \Delta w_2^{\,2} + \Delta P_{tie}^{\,2} + \Delta u_1^{\,2} + \Delta u_2^{\,2} dt \qquad (19)$$

4) Based on the value of the performance index, use PSO as described in section 3, to generate new feedback gains and switching vector values.

5) Evaluate the performance index in step 2 for the new feedback gains and switching vector values. Stop if there is no more improvement in the value of the performance index or if the maximum number of iterations has been used, otherwise go to step 3.

These steps are illustrated in the flow-chart of Figure 4.

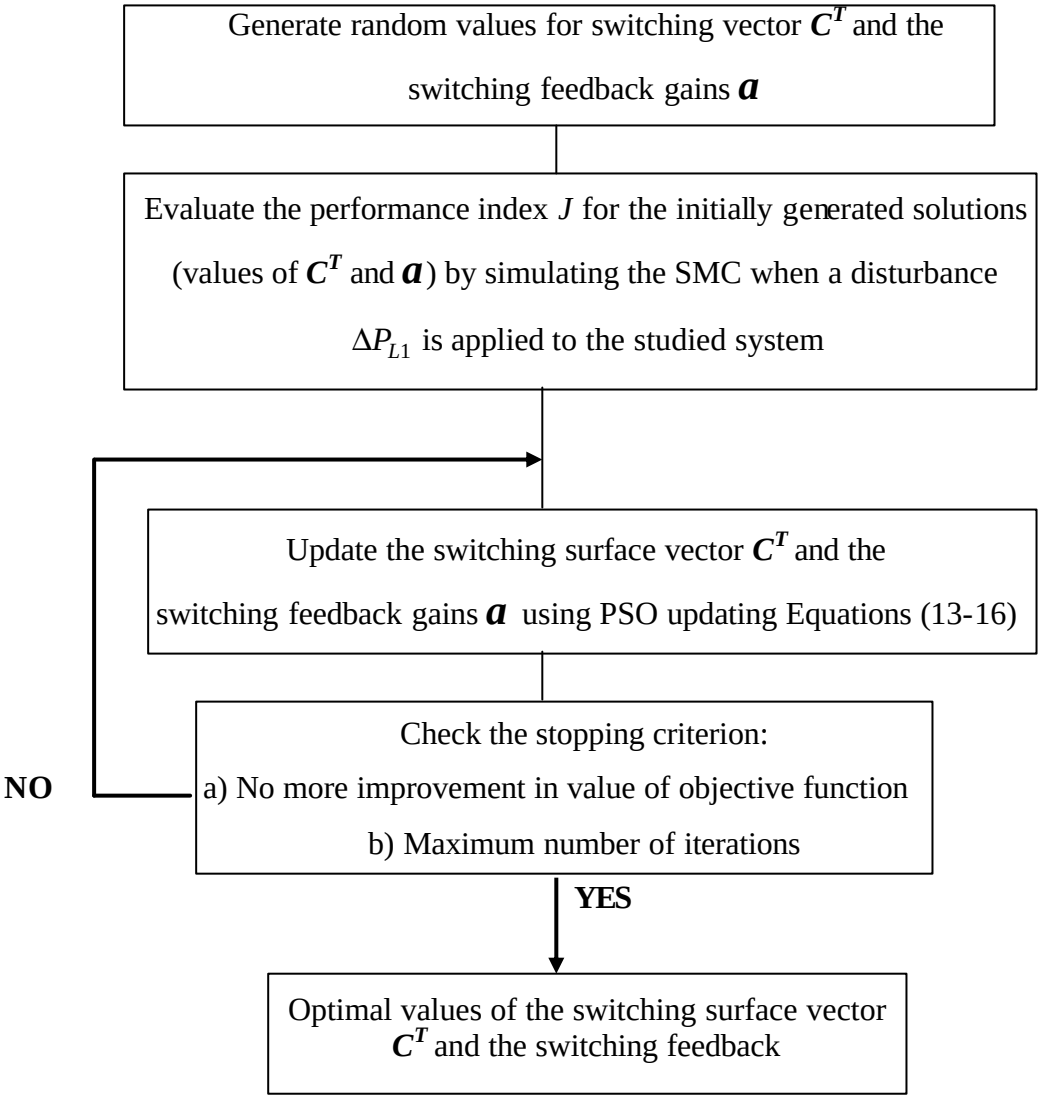

Figure 4: Optimal selection of the feedback gains and switching vectors using PSO

5. Simulation Results

The present design method will be compared with the one proposed by Yang and Cimen (1996) where a Linear Quadratic Regulator (LQR) based on structured singular values was presented in designing a robust AGC for two area interconnected nonlinear power systems. Yang and Cimen (1996) selected a conventional integral controller with unity gains. For comparison purposes, the present paper uses PSO for the selection of the

optimum gains of this integral controller. The present optimum gains are $K_1 = 0.5512$ and $K_2 = 0.01$.

The PSO settings used are: number of particles = 15, maximum number of iterations = 500, $w_{max} = 0.9$, $w_{min} = 0.4$, and the maximum velocity constant factor $k = 0.1$. On the other hand, for the SMC, the present optimum switching vector values and feedback gains were found to be as follows:

i) For objective function $\boldsymbol{J_1}$:

$\boldsymbol{C_1^T}$ =

30.0000	13.0638	4.8552	24.9203	17.8597	-3.0000	-3.0000	4.9979	-3.0000
12.0642	17.4207	3.4430	23.6198	13.0664	17.6442	30.0000	5.8677	18.7206

$\boldsymbol{a_1}$ =

3.3757	0.0010	4.5620	0.0010	7.4638	2.4800	0.0010	4.7885	1.2752
0.0010	0.0010	0.0010	1.8695	5.4026	5.5483	8.6752	0.0010	5.8926

ii) For objective function $\boldsymbol{J_2}$ **:**

$\boldsymbol{C_2^T}$ =

17.5282	23.4810	1.6520	16.5393	24.5775	6.4494	13.9074	7.1777	30.0000
13.5409	3.1294	2.8040	-2.8377	23.3587	2.0022	4.0492	12.0614	22.2385

$\boldsymbol{a_2}$ =

5.3594	0.0697	0.0010	5.0151	1.3586	0.0010	5.8891	4.3556	2.8171
0.0010	9.0000	0.0010	8.9998	5.8002	0.1515	0.1642	9.0000	9.0000

After getting the above SMC parameters, the system is simulated for a 0.01 p.u. load disturbance in area 1. The fast convergence of the objective functions J_1 and J_2 are shown in Fig. 5.

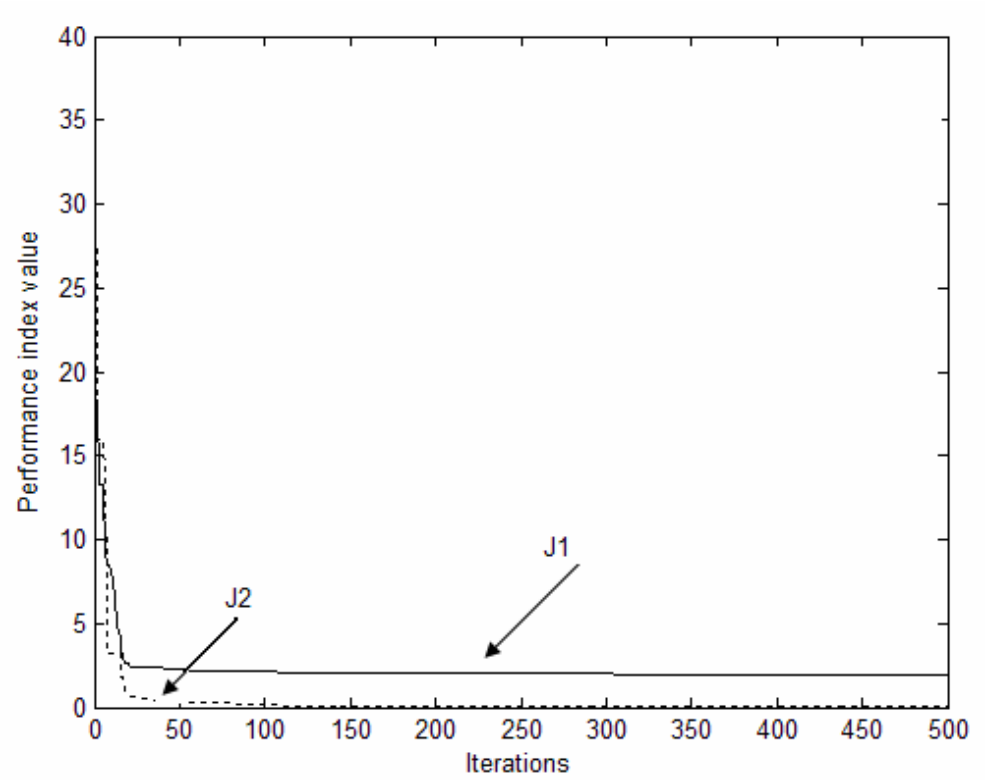

Fig. 5: Convergence of the two objective functions J_1 and J_2

The frequency deviation in areas 1 and 2 as well as the tie-line power change of the interconnected system ,as compared to the previous attempt reported in the literature (Yang and Cimen,1996) and the present optimal integral control, are shown in Figs. 6-8.

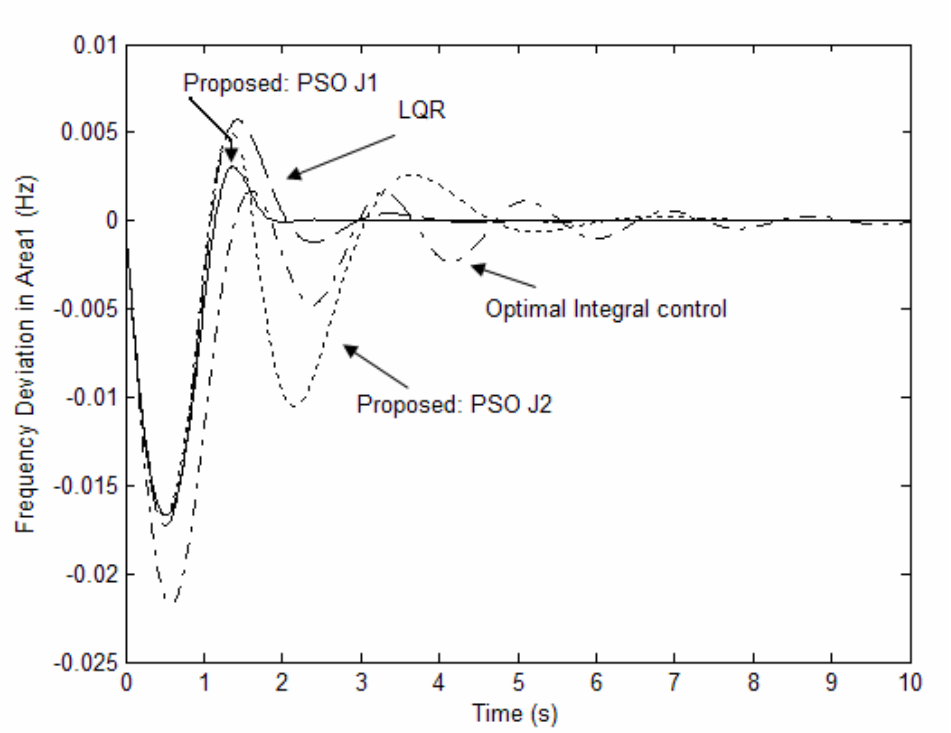

Fig. 6: Frequency deviation in area 1 when using proposed controllers and LQR controller (Yang and Cimen, 1996)

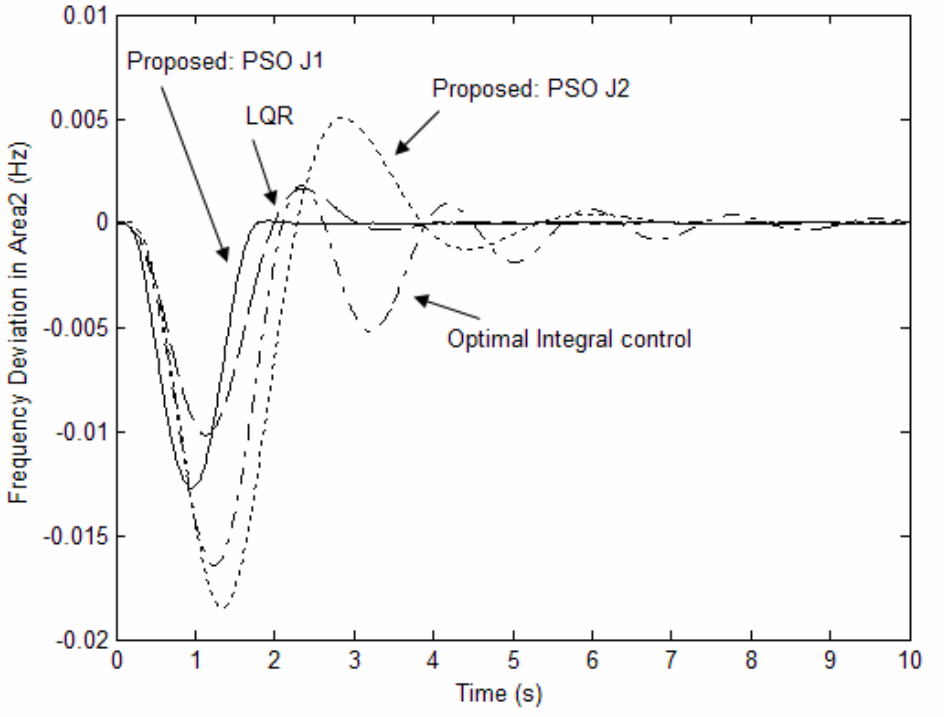

Fig. 7: Frequency deviation in area 2 when using proposed controllers and LQR controller (Yang and Cimen, 1996)

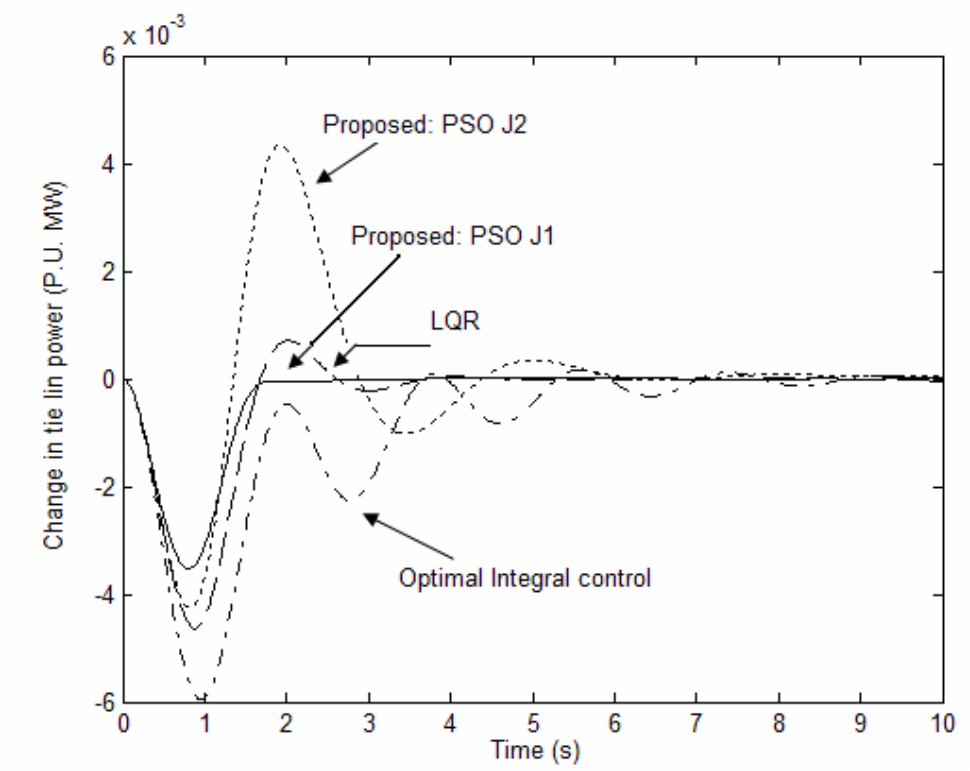

Fig. 8: Tie-line power deviation when using proposed controllers and LQR controller of (Yang and Cimen, 1996)

It is quite clear that using J_1 as a performance function allows the design of a SMC controller with improved dynamic behaviour, as seen in Figs. 6-8. This is on the expense of increased fluctuations (chattering) in the control efforts u_1 and u_2 as seen in Fig. 9. On the other hand, Fig. 10 shows that including the deviation of the control effort into the performance function as in J_2 reduced dramatically the chattering in the control signal (effort). This reduction in the chattering is on the expense of degradation (but still acceptable) in the dynamical behaviour of the interconnected systems as seen in the comparison of Figs. 6-8.

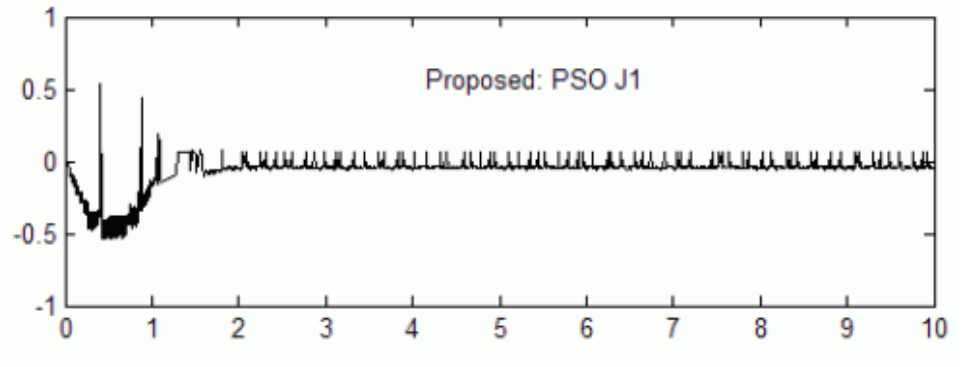

(a)

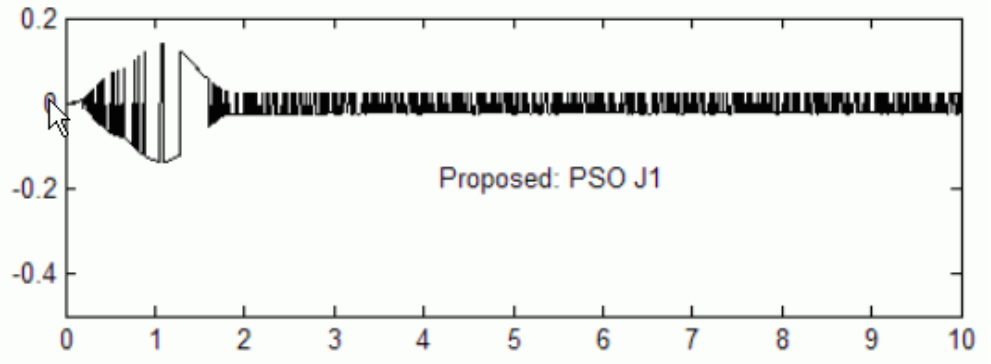

(b)

Fig. 9: Control signals (efforts) when using the objective function J_1: (a) u_1, (b) u_2

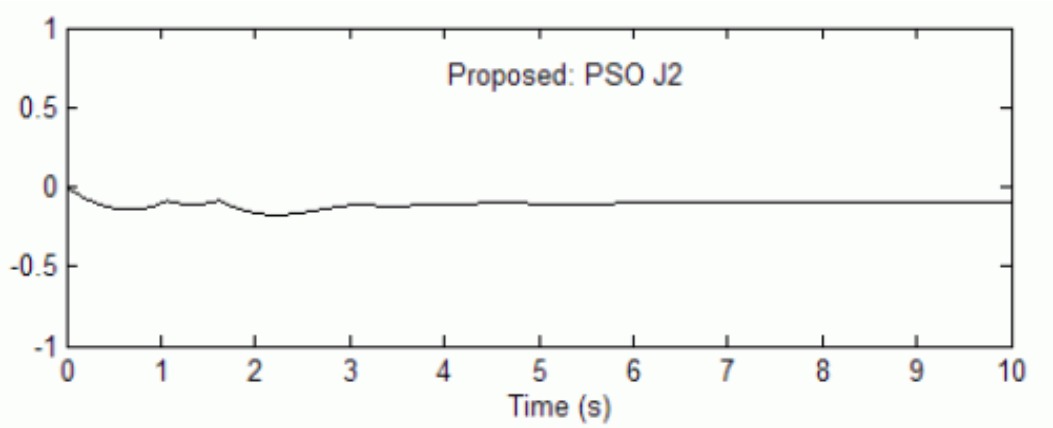

(a)

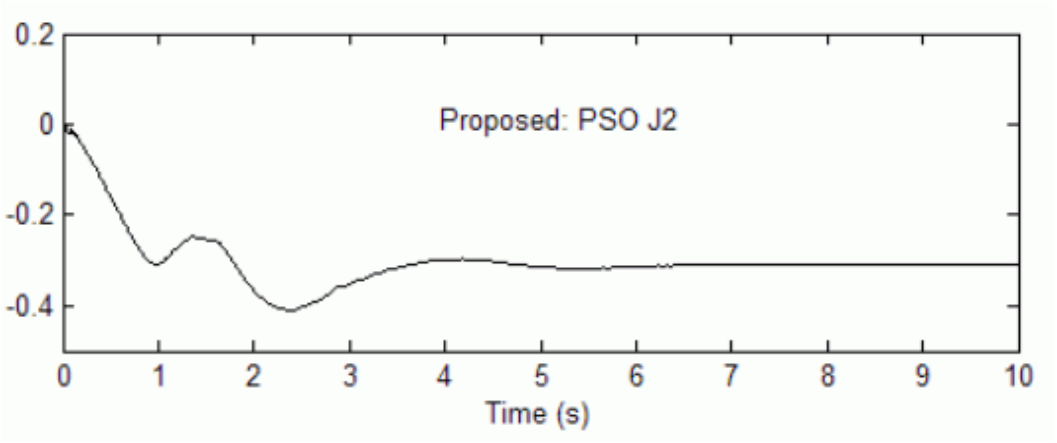

(b)

Fig. 10: Control signals (efforts) when using objective function J_2: (a) u_1, (b) u_2

In order to test the robustness of the proposed controllers, the model parameters T_{p1}, T_{p2}, T_{g1}, T_{g2}, K_{p1}, and K_{p2} were changed by $\pm 25\%$. The controller feedback gains and switching vector values obtained before when taking J_1 as an objective function are kept the same. The dynamical behaviour of the proposed controller under the 0.01 p.u. load disturbance in area 1 is shown in Figs. 11-13, for frequency deviation in areas 1, and 2 and the tie line power change, respectively. From these figures, it is quite clear that the controller has a satisfactory performance in terms of robustness against model parameter variations. The performance of the proposed SMC controller when J_2 was used showed a similar performance and hence not reported.

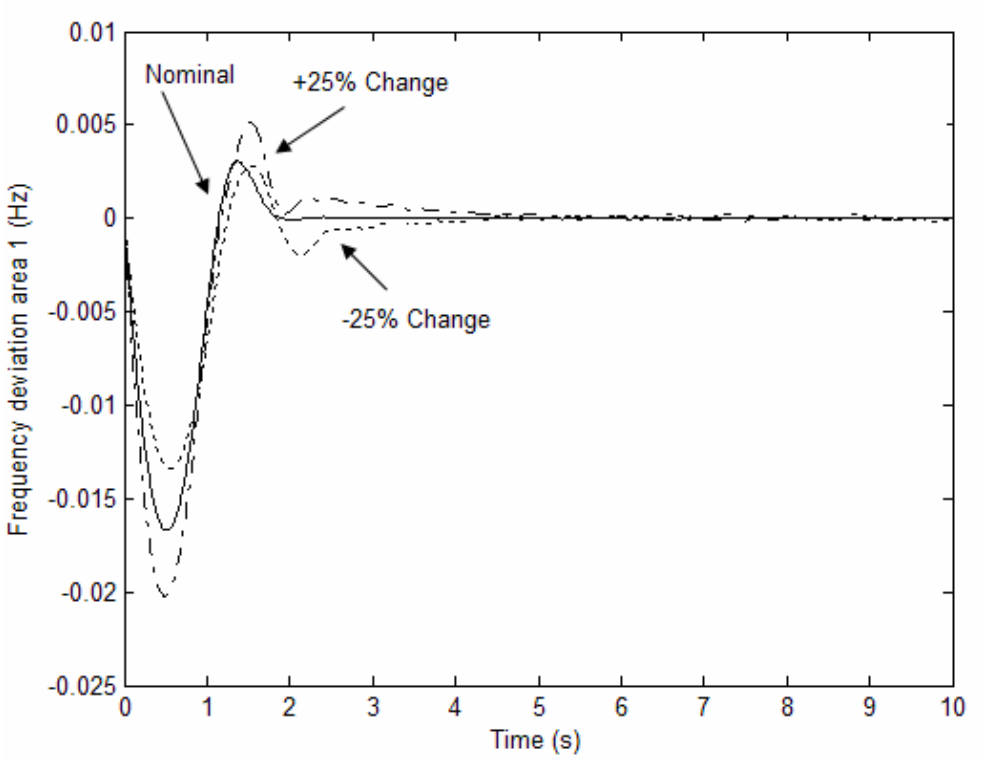

Fig. 11: Effect of system parameters variation on frequency deviation in area 1

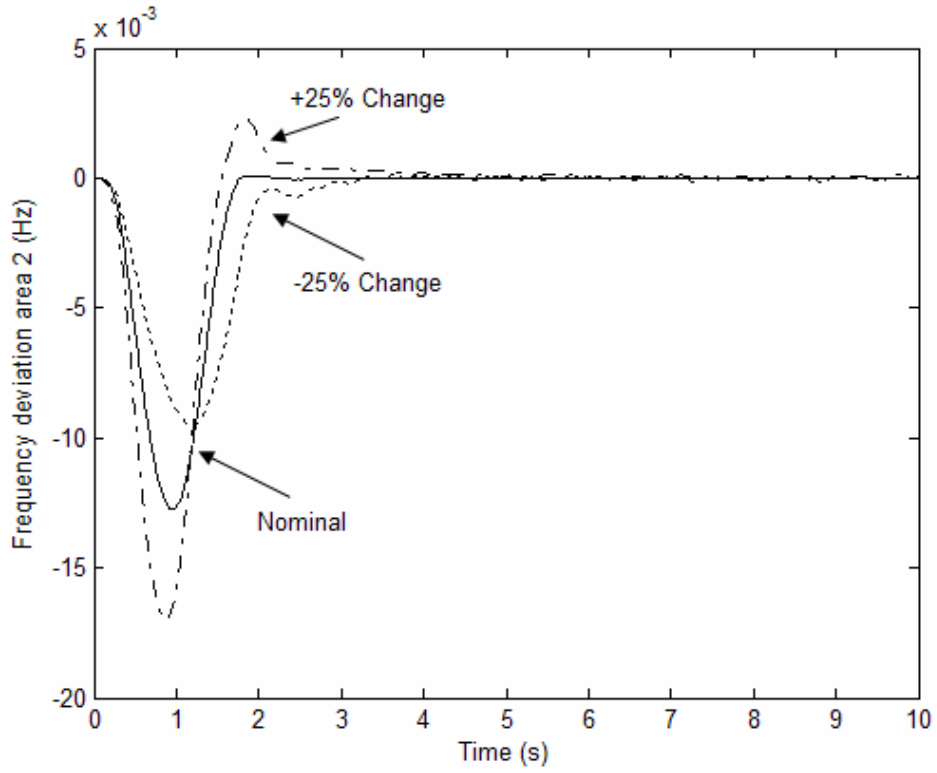

Fig. 12: Effect of system parameters variation on frequency deviation in area 2

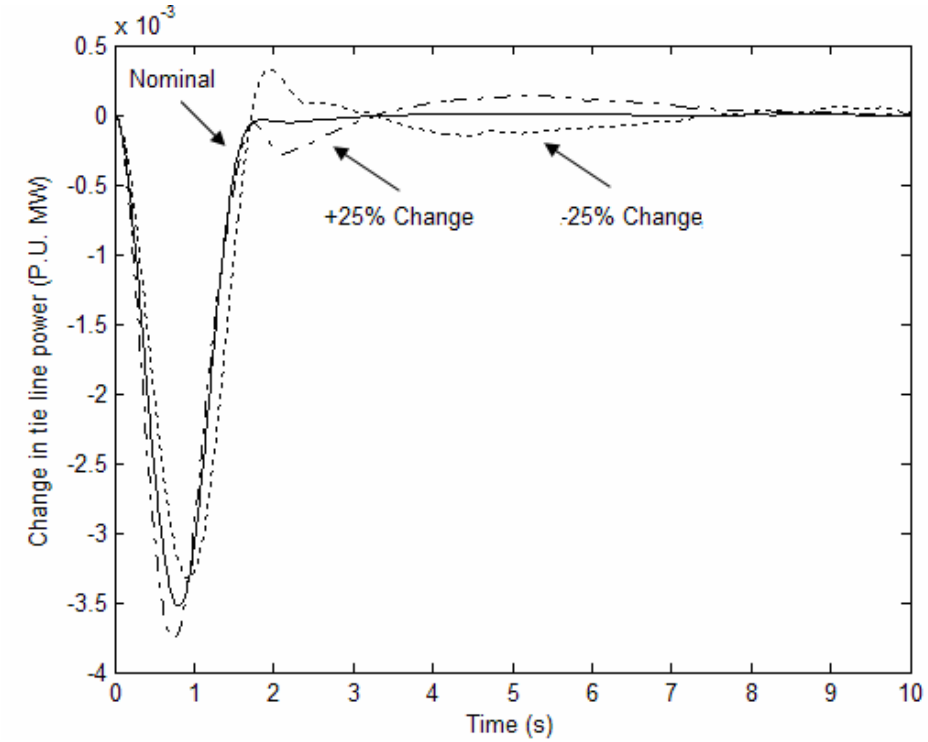

Fig. 13: Effect of system parameters variation on tie-line power deviation

In order to investigate the effect of varying the GRC values on the designed controller robustness, the controller has been tested for different values of GRC and the results of frequency deviation are shown in Figure 14. This figure demonstrates that the designed controller can perform satisfactorily under a wide range of GRC values.

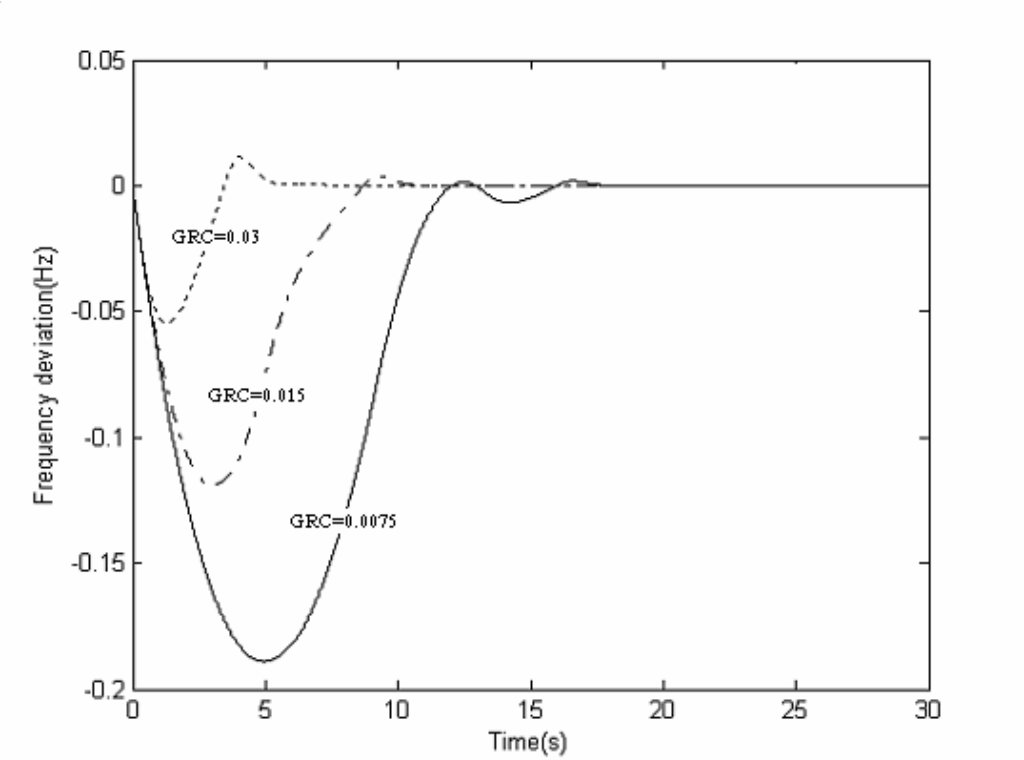

Fig. 14: Effect of changing GRC values on frequency deviation

6. Conclusions

An efficient sliding mode controller has been designed with a chattering reduction feature. The optimal feedback gains and switching vector values of the controller are selected based on formulating the SMC design procedure as an optimization problem. Particle swarm optimization algorithm is used as an optimization tool.

The proposed controller has been applied effectively on a practical two-area AGC problem with nonlinearities in the model. The dynamical performance of the system when using the proposed controller is highly enhanced as compared to the dynamics when using previous controllers. The chattering in the control efforts had been successfully eliminated using a new performance function. In addition, the proposed controller has been found to be robust against parameter variations of the model.

Acknowledgment

The authors would like to acknowledge the support of King Fahd university of Petroleum and Minerals.

References

Al-Hamouz, Z., Al-Duwaish, H., 2000. A new load frequency variable structure controller using Genetic algorithms. Electric Power Systems Research 55 (1), 1-6.

Al-Hamouz, Z., Al-Duwaish, H., Al-Musabi, N., 2007. A Tabu Search Approach for the Design of Variable Structure Load Frequency Controller Incorporating Model Nonlinearities. JEEEC 58 (5), 264-270.

Al-Hamouz, Z., Al-Musabi, N., Al-Duwaish, H., Al-Baiyat, S., 2005. On the Design of Variable Structure Load Frequency Controllers by Tabu Search Algorithm: Application to Nonlinear Interconnected Models. Electric Power Components and Systems 33 (6), 1253-1267.

Al-Musabi, N., Al-Hamouz, Z., Al-Duwaish, H., Al-Baiyat, S., 2003. Variable structure load frequency controller using the particle swarm optimization technique. Proc. of the 10th IEEE International Conference on Electronics, Circuits and Systems, 380-383.

Beaufays, F., Abdul-Magid, Y., Widrow, B., 1994. Applications of Neural Networks to load frequency control in power systems. Neural Networks, 7 (1), 183-194.

Benjamin, N. N., Chan, W.C., 1978. Multilevel Load-Frequency of interconnected power systems. Proc. IEE 125 (6), 521-526.

Chan, W.C., Hsu, Y.Y., 1981. Automatic generation control of interconnected power system using variable structure controllers. Proc. IEE Part C 128 (5), 269-279.

Demiroren, A., Sengor, N.S., Zeynelgil, H.L., 2001. Automatic generation control by

using ANN technique. Electric Power Components and Systems 29 (10), 883-896.

Demiroren, A., Zeynelgil, H.L., Sengor, N.S., 2003. Automatic generation control for power system with SMES by using Neural Network controller. Electric Power Components and Systems 31 (6), 1-25.

Elgerd, O. I., Fosha, C.E., 1970. Optimum megawatt frequency control of multiarea electric energy systems. IEEE Trans. Power Appar. and Syst. PAS-89 (4), 556-563.

Glover, J.D., Schweppa, F. C., 1972. Advanced Load Frequency Control. IEEE Trans. Power Appar. and Syst. PAS-91 (3), 2095-2103.

Itkis, V., 1976. Control systems of variable structure. Keter Publishing House, Jerusalem

Kumar, I.P., Kothari, D.P., 2005. Recent philosophies of automatic generation control strategies in power systems. IEEE Transactions on Power Systems 20 (1), 346–357.

Kennedy, J., Eberhart, R., 1995. Particle swarm optimization. IEEE International Conference on Neural Networks, 1942 -1948.

Kundur, P., 1994. Power System Stability and Control. McGraw-Hill, New York.

Moon, Y.H., Ryu, H.S., Kook B-K. C-H., 1999. Improvement of system damping by using differential feedback in the load frequency control. Proc. Of the IEEE PES 1999 Winter Meeting, 683-688.

Nanda J., Kaul., B. L., 1978. Automatic generation control of an interconnected power system. Proc. IEE 125 (5), 385-390.

Rerkpreedapong, D., Feliachi, A., 2003. PI gain scheduler for Load frequency control using spline techniques. Proc. of the 35th southeastern symposium on system theory, 259-263.

Sivarmakrishnan, A.Y., Hariharan, M.V., Srisailam, M.C., 1984. Design of variable structure load frequency controller using pole assignment technique. Int. Journal Control 40 (3), 487-498.

Utkin, V., Yang, K., 1978. Methods for constructing discontinuity planes in multidimentional variable structure systems. Autom. and Remote Control 39, 1466-1470.

Velusami, S., Chidambaram, I., 2006. Design of decentralized biased dual mode controllers for load frequency control of interconnected power systems. Electric Power Components and Systems 34 (3), 1057-1075.

Yang, T.C., Cimen, H., 1996. Applying structured singular values and a new LQR design to robust decentralized power system load frequency control. Proceedings of the IEEE international conference on industrial technology, 880-884.

.

Figures Caption